

Spectral Sequence Motif Discovery

Nicoló Colombo¹ and Nikos Vlassis²

¹nicolo.colombo@uni.lu, Luxembourg Center for Systems Biomedicine, University of
Luxembourg

²vlassis@adobe.com, Adobe Research, San Jose, CA*

November 21, 2021

ABSTRACT. Sequence discovery tools play a central role in several fields of computational biology. In the framework of Transcription Factor binding studies, motif finding algorithms of increasingly high performances are required to process the big datasets produced by new high-throughput sequencing technologies. Most existing algorithms are computationally demanding and often cannot support the large size of new experimental data. We present a new motif discovery algorithm that is built on a recent machine learning technique, referred to as Method of Moments. Based on spectral decompositions, this method is robust under model misspecification and not prone to locally optimal solutions. We obtain an algorithm that is extremely fast and designed for the analysis of big sequencing data. In few minutes, we can analyse datasets of more than hundred thousand sequences and produce motif profiles that match those computed by various state-of-the-art algorithms.

1 Introduction

In the last decades, due to the advent of new sequencing technologies, motif discovery algorithms have become an essential tool in many computational biology fields. In cell biology, sequence motif discovery plays a primary role in the understanding of gene expression through the analysis of sequencing data and the identification of DNA-transcription factors binding sites [1, 2, 3, 4, 5, 6].

Various experimental techniques are nowadays available to extract DNA-protein binding sites in-vivo (CHip-Seq [7]) and in-vitro (PBM [8], HT-SELEX [9, 10, 11, 12]). Thanks to the quantity and quality of

*The bulk of this work was carried out when NV was with the Luxembourg Centre for Systems Biomedicine.

data produced, HT-SELEX is considered one of the most promising high-throughput techniques for studying transcription factors binding affinity in-vitro (see the recent work [13] for a quantitative comparison between HT-SELEX and other high-throughput techniques as CHip-seq and PBM). In the HT-SELEX protocol, tens of thousands enriched DNA fragments are obtained through a series of incubation/selection cycles. In each cycle, an initial pool containing randomised ligands of length 14-40 bp is incubated with an immobilised DNA-binding protein. Bounded ligands are amplified by PCR, sequenced and then used as initial pool for a next cycle, until the pool is saturated [9, 10, 14, 11, 12].

Due to the high but not exact specificity of transcription factors binding affinities, enriched DNA fragments in a dataset typically contain similar but not exactly conserved instances of the same binding motif. Sequence discovery algorithms are required to produce binding models that are at the same time intuitively clear and able to capture the full complexity of such probabilistic mechanisms [14, 11, 8]. In the simplest case, binding preferences are reported using consensus sequences, obtained by selecting a few deterministic character strings that are over-represented in the dataset. A more flexible representation is provided by Position Weight Matrices (PWM) that describe binding sites as probability densities over the DNA alphabet. Based on the stringent assumption that the total binding energy is a site-by-site sum of single protein-nucleobase interactions, PWM's are only approximate models of the true transcription factor preferences. A debate is still open on whether such approximation gives a satisfactory picture of the DNA-proteins interaction or is a too simplified reduction of the real biological process [15]. More sophisticated models, that go beyond the PWM representation by taking into account multiple bases probability distributions or long-distance interactions, have been proposed and tested in the literature [16, 17, 15, 18, 19]. However, in most cases, these improvements could not provide any evidence against the simpler and more intuitive approach based on position independent distributions [20].

In machine learning, factorized (aka product) distributions like PWMs and their linear combinations (aka mixtures) are commonly used in modelling empirical distributions from various kinds of data. The problem of learning mixtures of product distributions from given datasets has been intensively studied [21, 22]. In particular, as proposed by Chang (1996), it is possible to infer a mixture of product distributions via the spectral decomposition of 'observable' matrices, *i.e.* matrices that can be estimated directly from the data using suitable combinations of the empirical joint probability distributions [23]. Extensions and improvements of this idea have been developed more recently in a series of remarkable works, where the spectral technique is applied to a larger class of probability distributions, and robust versions of the original method have been analysed theoretically [24, 25, 26, 27].

In this paper, we further develop the original spectral technique [23] and study its application to the problem of learning probabilistic motif profiles from noisy sequencing data. The key observation is that, in

the PWM approximation, motif discovery reduces to the more general issue of learning a mixture of product distributions and hence it is possible to extract motif profiles from sequencing data using usual spectral decompositions. In particular, we combine some of the improvements introduced in [24] and [28, 27] to obtain a more stable spectral decomposition and implement a few new ideas to adapt the general technique to the DNA sequence discovery problem. Through this work, we always assume that transcription factors specificities are well described by product distributions *i.e.* PWM's, and leave for future work the spectral inference of more advanced motif representations.

The paper is organised as follows: in Section 2 we give a brief overview of some related works, in Section 3 we describe the spectral methods and their applications to sequencing datasets and in Section 4 we summarize our main results. More mathematical details about the spectral techniques can be found in Appendix A and a schematic version of our algorithm is provided in Appendix B. A software implementation of our method is available under request at `nicolo.colombo@uni.lu`.

2 Related Work

Motif Finding The literature on sequence motif discovery is vast. We refer to [29, 30, 31, 32] for reviews and additional references. There are two main classes of motif finding algorithms, probabilistic and word-based. Probabilistic algorithms search for the most represented un-gapped alignments in the sample to obtain deterministic consensus sequences, PWM models, or more advanced models that take into account multi-base correlations [16, 17, 15, 18, 19]. Word-based algorithms search the dataset for deterministic short words, measure the statistical significance of small variations from a given seed, or transform motif discovery into a kernel feature classification problem [33, 34, 35]. Our method and two of the algorithms we have used for evaluating our results, namely MEME [36] and STEME [37], belong to the probabilistic class, while the method used in [12] and DREME [38] are word-based algorithms. The latter algorithms can also compute PWM models, so it is of interest to compare algorithms of different classes (See Results section).

Spectral Methods Spectral methods have been applied as an alternative to the Expectation Maximization algorithm [39] for inferring various kinds of probability distributions, such as mixtures of product distributions, Gaussian mixtures, Hidden Markov models, and others [23, 24, 26, 27, 40, 27, 41] (see [42] for a recent review). These methods are not as flexible as the Expectation Maximization algorithm, but they are not prone to local optima and have polynomial computational time and sample complexity. Various spectral decomposition techniques have been proposed: Chang's spectral technique of [23, 24], the symmetric ten-

sor decomposition presented in [27], and an indirect learning methods for inferring the parameter of Hidden Markov Models [26]. The practical implementation of the spectral idea is a nontrivial task because the stability of spectral decomposition strongly depends on the spacing between the eigenvalues of the empirical matrices. In [24, 27] certain eigenvalue separation guarantees for Chang’s spectral technique are obtained via the contraction of the higher (order three) moments to Gaussian random vectors. In the tensor approach presented in [27], the non-negativity of the eigenvectors is ensured by using a deflating power method that generalizes usual deflation techniques for matrix diagonalization to the case of symmetric tensors of order three. A third possibility involves replacing the random vector of Chang’s spectral technique with an ‘anchor observation’ that, for each hidden state, ‘tends to appear in the state much more often than in the other states’ [43] and guarantees the presence of at least one well separated eigenvalue [44, 43]. Finally, as briefly mentioned in [27, 45], the stability of Chang’s technique can be significantly improved through the simultaneous diagonalization of several random matrices. Here, we present a new approach based on the simultaneous Schur triangularization of a set of nearly commuting matrices [28].

Spectral Method and Sequence Analysis To the best of our knowledge, spectral methods have not been applied so far to the problem of DNA sequence motif discovery that we address here. Nevertheless, spectral techniques have been applied to other types of sequence analysis problems, such as poly(A) motif prediction [46], chromatin annotation [43], and sequence prediction [47]. The techniques used in these works are all based, with minor modifications, on the spectral algorithm of Hsu et al. [26] for learning Hidden Markov Models, in which a dataset of time-series of observed values $\{x_1, x_2, \dots\}$ is used to recover a single observation matrix (O_x) whose columns are the conditional probabilities associated with the hidden states. Our approach marks a significant departure from these methods by allowing the recovery of distinct observation matrices (O_x, O_y, \dots) and hence the extraction of motif PWM’s. Finally, we note that a general technique for learning mixture of product distributions in the presence of a background has been recently presented [48]; it would be interesting to study how this technique could be applied to the problem of sequence motif discovery.

3 Methods

DNA-protein interactions can be approximated by PWM models under the assumption that the total binding energy is the sum of single protein-nucleobase interactions. In this case, Transcription Factors binding affinities are represented by $d \times \ell$ frequency matrices, where d is the dimensionality of the sequences alphabet and ℓ the length of the binding site. Looking at these frequency matrices as components of a mixture

of product distributions, we recover all their entries via the spectral decomposition of "observable" matrices computed from data.

To obtain the empirical distributions we use a length- ℓ sliding window that runs over all sequences in the dataset with one-character steps. We take into account the possible presence of secondary motifs by considering mixtures with high number of components. This choice is also motivated by the fact that the one-character steps of the sliding window can produce strong signals for many shifted versions of the same sub-sequences. In practice, if p is the number of components in the mixture we set $p > 15$ and select the $p_{\text{top}} \sim 3$ most informative components at the end, according to their relative entropy respect to a background distribution. Moreover, since spectral techniques do not apply when the number of mixture components is higher than the dimension of the sequence alphabet, we augment the size of the sequences space by grouping contiguous variables and work with an alphabet of higher dimensionality. Concretely, letting d be the dimensionality of the sequence alphabet \mathcal{A} and n the number of variables in a group, the corresponding grouped variables have dimensionality d^n and take values in the alphabet $\mathcal{A}^{\otimes n}$. For example, if x_1, \dots, x_ℓ are the single character variables of a length- ℓ sliding window $W = [x_1, \dots, x_\ell]$, we consider three grouped variables $x = [x_1, \dots, x_n]$, $y = [x_{n+1}, \dots, x_{2n}]$, $z = [x_{2n+1}, \dots, x_\ell]$ such that $W = [x, y, z]$.

Assuming for simplicity a mixture of product distributions with $p = d^n$ hidden components defined over a d^n -dimensional space, pairwise and triple probability tensors read

$$[P(x, y)]_{ij} = \sum_{r=1}^p h_r X_{ir} Y_{jr}, \quad [P(x, y, z)]_{ijk} = \sum_{r=1}^p h_r X_{ir} Y_{jr} Z_{kr} \quad i = 1, \dots, d^n \quad (1)$$

where $[P(x)]_i$ is the probability of observing $x = i$, the mixing weights h_r satisfy $0 < h_r < 1$ and $\sum_r h_r = 1$ and X, Y, Z are $d^n \times p$ matrices that contain the conditional probability distributions, for variables x, y, z respectively. For any d^n -dimensional vector θ one has

$$[P_\theta(x, y, z)]_{ij} = \sum_k [P(x, y, z)]_{ijk} \theta_k = [X \text{diag}(h) \text{diag}(\theta^T Z) Y^T]_{ij} \quad (2)$$

where $\text{diag}(h)$ and $\text{diag}(\theta^T Z)$ are $p \times p$ diagonal matrices whose entries are the components of $h = [h_1, \dots, h_p]$ and $\theta^T Z$ respectively. If the conditional probability matrices X, Y have both rank p and $h_r > 0$ for all $r = 1, \dots, p$, from (1) and (2) one obtains the matrix

$$S(\theta) = P_\theta(x, y, z) (P(x, y))^{-1} = X \text{diag}(\theta^T Z) X^{-1} \quad (3)$$

that is called 'observable' because its empirical estimation, say $\hat{S}(\theta)$, can be directly obtained from the sequences sample, using the joint empirical probabilities $\hat{P}(x, y)$ and $\hat{P}(x, y, z)$. When the dimensionality of the sequence alphabet d and the number of grouped variables n is big, the manipulation of the $d^n \times d^n$

empirical matrices can be computationally expensive. Moreover, it can be useful in general to learn a mixture with a smaller the number of mixture components $p < d^n$. This is obtained by reducing $\hat{S}(\theta)$ down to a $p \times p$ matrix through a rank- p approximation of the empirical distributions. More precisely, all empirical moments become $p \times p$ matrices after multiplication (from the left and from the right) with the transpose of suitable $d^n \times p$ rectangular matrices, formed with the first p (left and right) singular vectors of the empirical pairwise probabilities $\hat{P}(x,y)$ and $\hat{P}(x,z)$. See Appendix A for a formal definition of $\hat{P}(x,y)$ and $\hat{P}(x,y,z)$ and more details on their rank- p reduction.

In the case of misspecified models, *i.e.* when the sample is not drawn exactly from a mixture of product distributions with exactly p mixture components, $\hat{S}(\theta)$ can be identified only approximately with the right hand side of (3). Even in this case, it can be shown that the recovery of X and Z is theoretically possible, with certain success guarantees [24, 26, 25]. However, when the empirical moments are not exact, the stability of the spectral method depends strongly on the (real) separation between the eigenvalues of $\hat{S}(\theta)$. A theorem, *Lemma 4 (Eigenvalues separation)* in [24], proves that a sufficient separation is obtained with high probability if θ is chosen to be a random vector whose entries are independent Gaussians with mean 0 and variance 1. To increase further the stability of our algorithm, we define a set of distinct random vectors $\{\theta_1, \theta_2, \dots\}$ and simultaneously diagonalise the set of (nearly commuting) empirical matrices $\hat{S}(\theta_i)$. As suggested in [28], if $\hat{S}(\theta_i)$ for $i = 1, 2, \dots$ is a set of nearly commuting matrices and Q, σ are respectively the orthogonal and upper triangular matrices in the Schur decomposition of their linear combination $\hat{S} = \sum_i \hat{S}(\theta_i) = Q\sigma Q^T$, the approximate eigenvalues of each $\hat{S}(\theta_i)$ can be read from the diagonal of $\tilde{T}_i = Q^T \hat{S}(\theta_i) Q$. Since the matrices $\hat{S}(\theta_i)$ do not commute exactly, the triangularisation obtained via Q is approximate and \tilde{T}_i can contain small entries below the diagonal. It can be shown (see Appendix for details) that the size of such entries is proportional to $\varepsilon = \max_{i,j} \|\hat{S}(\theta_i)\hat{S}(\theta_j) - \hat{S}(\theta_j)\hat{S}(\theta_i)\|_F$, where $\|A\|_F = \sqrt{\text{Tr}[A^T A]}$, provided that the eigenvalues of \hat{S} are well separated. The error in the eigenvalues estimation can then be bounded via usual eigenvalues perturbation theorems, where the norm of the perturbation matrix is proportional to ε .

Thus, we choose a set of d^n -dimensional random vectors $\{\theta_1, \dots, \theta_p\}$ and form a $p \times p$ matrix Λ whose rows contain the approximate eigenvalues of the corresponding matrices $\hat{S}(\theta_i)$. The matrices Z is then computed from $Z = \Theta^{-1}\Lambda$, where Θ is a $p \times d^n$ matrix formed with the d^n -dimensional random vectors $\{\theta_1, \dots, \theta_p\}$. Finally we recover X and Y using the obtained Z to approximately diagonalise sets of analogous "observable" matrices, say $\hat{S}_x(\theta_i)$ and $\hat{S}_y(\theta_i)$, obtained from different combinations of the empirical moments, see Appendix A for more details.

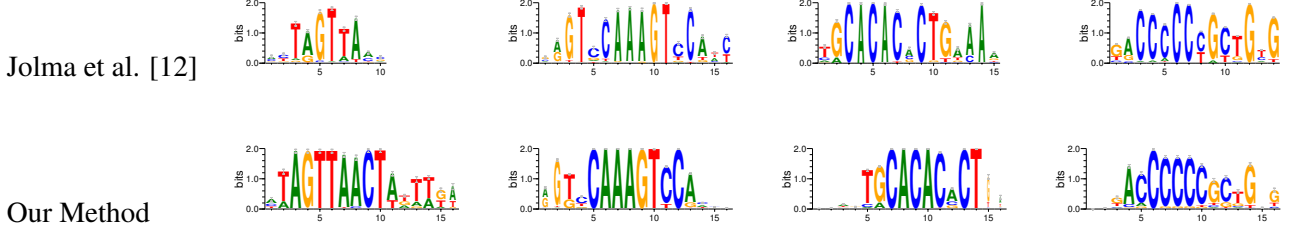


Figure 1: HMBOX1, HNF4A, ZSCAN4 and ZIC1 models published in [12] and models computed using our method on the same datasets.

Together, the matrices X, Y, Z combine to build a set of higher dimensional PWM's defined by

$$H_r \in [0, 1]^{d^m \times 3} \quad s.t. \quad \begin{cases} [H_r]_{i1} = X_{ir}, & [H_r]_{i2} = Y_{ir}, & [H_r]_{i3} = Z_{ir} \\ \sum_i [H_r]_{ik} = 1 & \forall k = 1, 2, 3 \end{cases} \quad (4)$$

for $r = 1, \dots, p$ and $i = 1, \dots, d^m$. To select the nontrivial mixture components H_r^{top} we compute, for each H_r , the relative entropy $I(r) = \sum_{j,k} [\frac{H_r}{B}]_{ij} \log[\frac{H_r}{B}]_{ik}$, where B is a background distribution obtained from a control dataset. In particular, the control dataset consists of sequences that come from a different transcription factor experiment and the background distribution is obtained from its empirical joint probability distributions (see Appendix A for more details). We choose the models of smallest relative entropy to create sub-sequences alignments and extract the final d -dimensional models h_r^{top} . For each $r = 1, \dots, p_{\text{top}}$, we define a scoring function using the log-likelihood of H_r^{top} and include in the alignment all length- ℓ sub-sequences whose score is above a certain threshold. The thresholds are chosen within a finite set of possible values¹, in order to maximise the small-sample corrected information content of the low-dimensional model h_r^{top} .

4 Results

We present a new motif finding algorithm that is faster than other sequence discovery tools and designed for processing noisy high-throughput dataset containing more than hundred thousand sequences. Based on a new and more stable implementation of spectral methods [23, 24, 26, 25], our algorithm is robust under model misspecification and is not prone to local optima. Moreover, our algorithm does not require any deterministic consensus sequence to initialize the search, and models are computed directly from the empirical joint frequency matrices. In addition, the method is completely general and, upon minor

¹We have used this heuristic approach since, in the case of probabilistic models, the problem of choosing an optimal matching threshold given a set of sequences has been proven to be NP-hard [49].

modifications, can be used for sequence discovery over any sequences alphabet and variable number and length of searched motifs, or adapted to analyse datasets with binding affinity scores [8, 7].

For testing our algorithm we have focused on the transcription factors binding affinity database associated to the recent work: *"DNA-Binding Specificities of Human Transcription Facotors"* by Jolma et al. [12] and available at the ENA database, under accession number ERP001824. All datasets consist of $\sim 10^5$ enriched genome fragments of length ~ 20 bp. For each transcription factor, we have download the dataset corresponding to the SELEX cycle used in [12] to compute the final model and run our algorithm on it. Since the amount of ligands with specific affinity is expected to increase in each cycle and saturate the pool after 4-5 cycle, PWM's are typically extracted from the third or fourth cycles.

We have used the frequency matrices published in the supplementary material of [12] to evaluate the quality of the models computed on the same data using our method. In Figure 1 we compare few logos obtained with our algorithm on the following datasets: HMBOX1 (cycle 4, 29156 sequences), HNF4A (cycle 4, 80491 sequences), ZSCAN4 (cycle 3, 68378 sequences) and ZIC1 (cycle 3, 267963 sequences). All logos have been computed using the application `weblogo 3.3` with no options [50], bash command

```
>weblogo -c classic <PWM.txt> PWM.eps (5)
```

where the file `PWM.txt` contains the $4 \times \ell$ frequency matrix, with ℓ being the length of the motif. The sum of the entries in each column equals the number of instances used for computing the frequency matrix. We have chosen this format because the PWM's computed by our algorithm and the PWM's published in [12] are already in this form.

We have then selected three other datasets, ELF3 (cycle 3, 78124 sequences), HNF1A (cycle 3, 142354 sequences) and MAFK (cycle 3, 144041 sequences), and run on each of them few other online available algorithms (MEME [36], DREME [38], STEME [37]). All algorithms ran with default settings but in many cases we had to reduce the input sequences file up to some maximum supported size, since none of them could handle files of the size of the original datasets. In figure 2 we compare the PWM's of [12] with the models obtained by our method (on the whole dataset) and by the other algorithms (on a random selection of the maximum supported size). It should be noted that logos computed on reduced samples are in surprisingly good agreement with the models of [12], computed on the whole dataset. Since all algorithms we have tried produce more than one motif for each dataset, we have selected for the comparison the most statistically relevant, according to the information provided by the various tools on the output page. Moreover, the PWM's obtained from the online output page of STEME, MEME and DREME are Position Specific Probability Matrix (PSPM), whose columns sum to one. For computing the logos using (5), we have transformed the PSPM to frequency matrices by multiplying each entry by the number of sites that

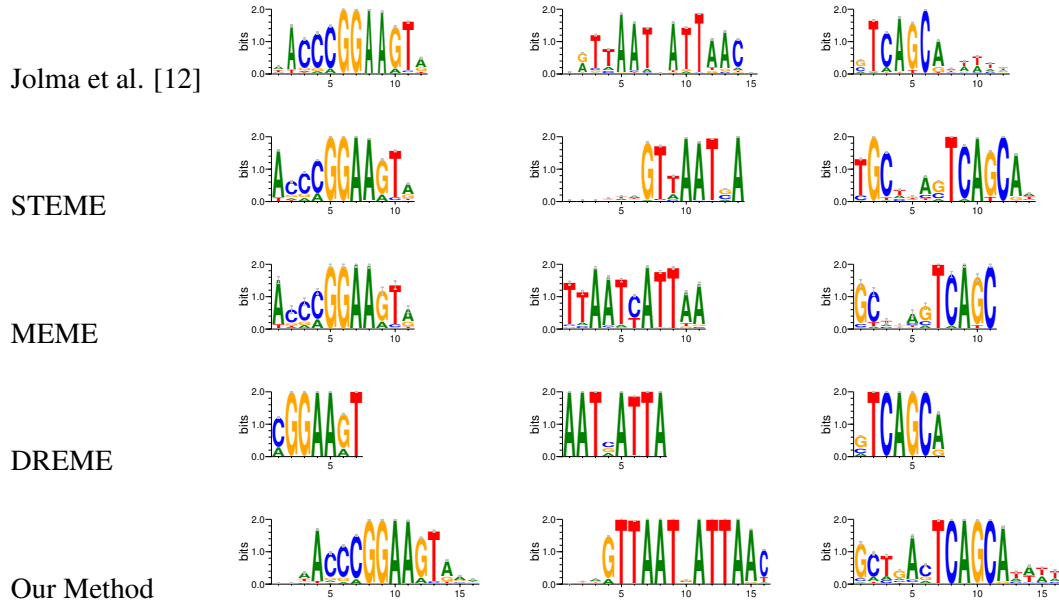


Figure 2: PWM computed by different algorithms on the ELF3, HNF1A and MAFK dataset from [12]. All logos were obtained using `weblogo 3.3` [50].

were included in the final alignment, as it appears on the first line of the output PSPM-format file. Except for DREME, that produces relatively short motifs ($\ell \leq 8$), the size of the motifs produced by all algorithms is similar and the typical range is $10 \leq \ell \leq 14$.

To compare the quality of the ELF3, HNF1 and MAFK logos we have computed the Area Under the ROC Curve (AUC) of each model on a series ground-truth test samples. For each transcription factor, the test samples consisted of 1000, 2000, 3000 4000, and 5000 positive instances, randomly selected from the transcription factor dataset, and an equal number of negative instances from a control dataset (we have used sequences from the ZIC1 dataset). Since motifs produced by different algorithms have different lengths, we have reduced their size down to the size of the shortest one by selecting the same 6-8 positions in the logo. We have defined the score function to be the maximum of the PWM's log-likelihood over all possible positions in the sequence and in its reverse complement. For each model, we have computed the AUC values associated to this score function on the five different test samples. In Figure 3 we report the average of the obtained AUC values and the corresponding standard variations. A possible problem of our AUC-test is the uncertainty about the ground-truth test sample, built on the (probably false) assumption that all sequences in a dataset come from effectively bounded DNA fragments.

Finally, we have compared the running times of the various algorithms on datasets of different sizes.

	DREME	Jolma et al. [12]	MEME	STEME	Our Method
ELF3	0.6171 (± 0.0102)	0.6331 (± 0.0116)	0.6353 (± 0.0125)	0.6367 (± 0.0136)	0.6373 (± 0.0141)
HNF1A	0.9818 (± 0.0016)	0.9819 (± 0.0017)	0.9832 (± 0.0009)	0.9788 (± 0.0014)	0.9794 (± 0.0019)
MAFK	0.6007 (± 0.0057)	0.5880 (± 0.0054)	0.6027 (± 0.0032)	0.5842 (± 0.0036)	0.6069 (± 0.0061)

Figure 3: Average AUC values for the logos shown in Figure 2. The average and standard variations are computed over five distinct tests, performed on different test samples containing the same amount of positives and negatives instances (respectively 2000, 4000, 6000, 8000 and 10000 sequences).

In Figure 4 (left) we show the execution times of DREME, MEME, STEME and our algorithm on sample containing respectively 3000, 6000, 12500, 25000 and 50000 randomly selected sequences of the HNF1A dataset. For all transcription factors and all dataset sizes our method has been the fastest and DREME the second fastest algorithm. The running time differences between our method and the others dramatically increase as the size of the dataset grows, see Figure 4. We remark the unusual behaviour of STEME whose running times increase very rapidly for small dataset sizes and reach a plateau at a sample size of 12500. MEME has only two values in the plot of Figure 4 because the algorithm can only support input files containing up to 60000 characters, *i.e.* 3000 sequences of length 20 bp. We also report a more careful comparison between the running times of DREME and our algorithm on datasets coming from three different experiments (ELF3, HNF1A and MAFK). For five given sample sizes, respectively 6000, 12500, 25000, 37500 and 50000 sequences, we have plotted the average time over the three different datasets and the corresponding standard deviation as errorbars, see 4 (right). Unfortunately, we could not find any information about the running times of the algorithm used in [12].

5 Conclusions

Under the (reasonable) approximation that TF-DNA binding affinities are position-independent, the problem of finding the over-represented motifs in a set of genome sequences is equivalent to learning a mixture of product distributions. The inference of mixtures of product distributions is a well known problem in computer science, and powerful techniques have been developed to solve the problem using spectral decomposition techniques. We have applied this idea to the problem of transcription factor binding motif discovery and developed an efficient fast motif discovery algorithm that computes globally optimal solutions and can support input datasets in the order of hundreds of thousand sequences. We have tested our method on HT-Selex experimental data and our algorithm produces PWM's that match the profiles obtained

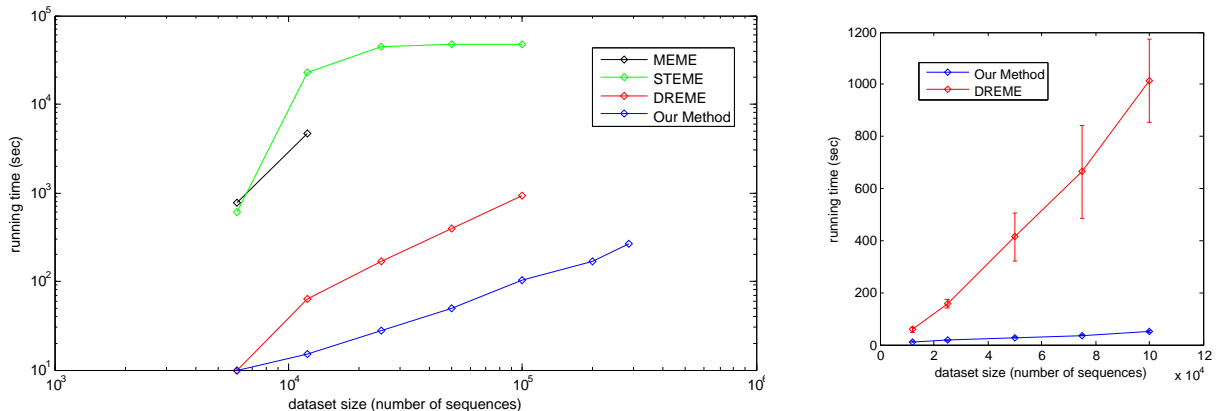


Figure 4: Left: Running times for various algorithms plotted against the dataset size (all algorithms ran on the HNF1A dataset of [12]); Right: Running times for our algorithm and DREME are plotted against the size of the datasets. Each point and corresponding errorbar represent respectively the average time and the standard deviation over three different runs, on the ELF3, HNF1A and MAFK datasets of [12] respectively.

by the state-of-the-art motif finding algorithms, but orders of magnitude faster. Future developments include the extension of our method to transcription factors binding models that go beyond the PWM approximation, and corresponding theoretical analysis.

Acknowledgments

We would like to thank Anke Wienecke-Baldacchino, Merja Heinaniemi, Matthieu Sainlez, Luis Salamanca and especially Cédric Laczny for useful discussions, comments and questions. This work was supported by FNR-Luxembourg CORE grant 12/BM/3971381 HIBIO.

References

- [1] M. F. Berger, A. A. Philippakis, A. M. Qureshi, F. S. He, P. W. Estep, and M. L. Bulyk, “Compact, universal DNA microarrays to comprehensively determine transcription-factor binding site specificities,” *Nature Biotechnology*, vol. 24, pp. 1429–1435, Nov. 2006.

- [2] G.-H. Wei, G. Badis, M. F. Berger, T. Kivioja, K. Palin, M. Enge, M. Bonke, A. Jolma, M. Varjosalo, A. R. Gehrke, J. Yan, S. Talukder, M. Turunen, M. Taipale, H. G. Stunnenberg, E. Ukkonen, T. R. Hughes, M. L. Bulyk, and J. Taipale, “Genome-wide analysis of ETS-family DNA-binding in vitro and in vivo,” *The EMBO Journal*, vol. 29, pp. 2147–2160, July 2010.
- [3] Z. Zhang, C. W. Chang, W. Hugo, E. Cheung, and W.-K. Sung, “Simultaneously learning DNA motif along with its position and sequence rank preferences through expectation maximization algorithm,” *Journal of Computational Biology*, vol. 20, pp. 237–248, Mar. 2013.
- [4] Y. Zhao, S. Ruan, M. Pandey, and G. D. Stormo, “Improved models for transcription factor binding site identification using nonindependent interactions,” *Genetics*, vol. 191, pp. 781–790, July 2012.
- [5] M. Annala, K. Laurila, H. Lahdesmaki, and M. Nykter, “A linear model for transcription factor binding affinity prediction in protein binding microarrays,” *PLoS ONE*, vol. 6, p. e20059, May 2011.
- [6] Q. Cheng, M. Kazemian, H. Pham, C. Blatti, S. E. Celniker, S. A. Wolfe, M. H. Brodsky, and S. Sinha, “Computational identification of diverse mechanisms underlying transcription factor-DNA occupancy,” *PLoS Genetics*, vol. 9, p. e1003571, Aug. 2013.
- [7] D. S. Johnson, A. Mortazavi, R. M. Myers, and B. Wold, “Genome-wide mapping of in vivo protein-DNA interactions,” *Science*, vol. 316, pp. 1497–1502, June 2007.
- [8] M. F. Berger and M. L. Bulyk, “Universal protein-binding microarrays for the comprehensive characterization of the DNA-binding specificities of transcription factors,” *Nature Protocols*, vol. 4, pp. 393–411, Mar. 2009.
- [9] C. Tuerk and L. Gold, “Systematic evolution of ligands by exponential enrichment: RNA ligands to bacteriophage t4 DNA polymerase,” *Science*, vol. 249, pp. 505–510, Aug. 1990.
- [10] K. W. Kinzler and B. Vogelstein, “The GLI gene encodes a nuclear protein which binds specific sequences in the human genome.,” *Molecular and cellular biology*, vol. 10, no. 2, pp. 634–642, 1990.
- [11] A. Jolma, T. Kivioja, J. Toivonen, L. Cheng, G. Wei, M. Enge, M. Taipale, J. M. Vaquerizas, J. Yan, M. J. Sillanpaa, M. Bonke, K. Palin, S. Talukder, T. R. Hughes, N. M. Luscombe, E. Ukkonen, and J. Taipale, “Multiplexed massively parallel SELEX for characterization of human transcription factor binding specificities,” *Genome Research*, vol. 20, pp. 861–873, June 2010.

- [12] A. Jolma, J. Yan, T. Whittington, J. Toivonen, K. R. Nitta, P. Rastas, E. Morgunova, M. Enge, M. Taipale, G. Wei, K. Palin, J. M. Vaquerizas, R. Vincentelli, N. M. Luscombe, T. R. Hughes, P. Lemaire, E. Ukkonen, T. Kivioja, and J. Taipale, “DNA-binding specificities of human transcription factors,” *Cell*, vol. 152, pp. 327–339, Jan. 2013.
- [13] Y. Orenstein and R. Shamir, “A comparative analysis of transcription factor binding models learned from PBM, HT-SELEX and ChIP data,” *Nucleic Acids Research*, vol. 42, pp. e63–e63, Apr. 2014.
- [14] Y. Zhao, D. Granas, and G. D. Stormo, “Inferring binding energies from selected binding sites,” *PLoS Computational Biology*, vol. 5, p. e1000590, Dec. 2009.
- [15] G. Badis, M. F. Berger, A. A. Philippakis, S. Talukder, A. R. Gehrke, S. A. Jaeger, E. T. Chan, G. Metzler, A. Vedenko, X. Chen, H. Kuznetsov, C.-F. Wang, D. Coburn, D. E. Newburger, Q. Morris, T. R. Hughes, and M. L. Bulyk, “Diversity and complexity in DNA recognition by transcription factors,” *Science*, vol. 324, pp. 1720–1723, June 2009.
- [16] M. L. Bulyk, “Nucleotides of transcription factor binding sites exert interdependent effects on the binding affinities of transcription factors,” *Nucleic Acids Research*, vol. 30, pp. 1255–1261, Mar. 2002.
- [17] X. Chen, T. R. Hughes, and Q. Morris, “RankMotif++: a motif-search algorithm that accounts for relative ranks of k-mers in binding transcription factors,” *Bioinformatics*, vol. 23, pp. i72–i79, July 2007.
- [18] M. Santolini, T. Mora, and V. Hakim, “Beyond position weight matrices: nucleotide correlations in transcription factor binding sites and their description,” *ArXiv e-prints*, Feb. 2013.
- [19] A. Mathelier and W. W. Wasserman, “The next generation of transcription factor binding site prediction,” *PLoS Computational Biology*, vol. 9, p. e1003214, Sept. 2013.
- [20] Y. Zhao and G. D. Stormo, “Quantitative analysis demonstrates most transcription factors require only simple models of specificity,” *Nature Biotechnology*, vol. 29, pp. 480–483, June 2011.
- [21] D. M. Titterton, *Statistical analysis of finite mixture distributions*. Wiley series in probability and mathematical statistics, Chichester ; New York: Wiley, 1985.
- [22] B. G. Lindsay, “Mixture models: theory, geometry and applications,” in *NSF-CBMS regional conference series in probability and statistics*, pp. 1–163, JSTOR, 1995.

- [23] J. T. Chang, “Full reconstruction of markov models on evolutionary trees: identifiability and consistency,” *Math Biosci*, vol. 137, pp. 51–73, Oct. 1996.
- [24] E. Mossel and S. Roch, “Learning nonsingular phylogenies and hidden markov models,” *The Annals of Applied Probability*, vol. 16, pp. 583–614, May 2006.
- [25] A. Anandkumar, D. Hsu, and S. M. Kakade, “A method of moments for mixture models and hidden markov models,” *CoRR*, vol. abs/1203.0683, 2012.
- [26] D. Hsu, S. M. Kakade, and T. Zhang, “A spectral algorithm for learning hidden markov models,” *Journal of Computer and System Sciences*, vol. 78, no. 5, pp. 1460 — 1480, 2012.
- [27] A. Anandkumar, R. Ge, D. Hsu, S. M. Kakade, and M. Telgarsky, “Tensor decompositions for learning latent variable models,” *CoRR*, vol. abs/1210.7559, 2012.
- [28] R. M. Corless, P. M. Gianni, and B. M. Trager, “A reordered schur factorization method for zero-dimensional polynomial systems with multiple roots,” pp. 133–140, ACM Press, 1997.
- [29] M. Tompa, N. Li, T. L. Bailey, G. M. Church, B. De Moor, E. Eskin, A. V. Favorov, M. C. Frith, Y. Fu, W. J. Kent, V. J. Makeev, A. A. Mironov, W. S. Noble, G. Pavesi, G. Pesole, M. Regnier, N. Simonis, S. Sinha, G. Thijs, J. van Helden, M. Vandenbogaert, Z. Weng, C. Workman, C. Ye, and Z. Zhu, “Assessing computational tools for the discovery of transcription factor binding sites,” *Nature Biotechnology*, vol. 23, pp. 137–144, Jan. 2005.
- [30] M. K. Das and H.-K. Dai, “A survey of DNA motif finding algorithms,” *BMC Bioinformatics*, vol. 8, no. Suppl 7, p. S21, 2007.
- [31] G. Sandve, O. Abul, V. Walseng, and F. Drablos, “Improved benchmarks for computational motif discovery,” *BMC Bioinformatics*, vol. 8, no. 1, p. 193, 2007.
- [32] D. Simcha, N. D. Price, and D. Geman, “The limits of de novo DNA motif discovery,” *PLoS ONE*, vol. 7, p. e47836, Nov. 2012.
- [33] C. Leslie, E. Eskin, and W. S. Noble, “The spectrum kernel: a string kernel for SVM protein classification,” *Pac Symp Biocomput*, pp. 564–575, 2002.
- [34] J.-P. Vert, R. Thurman, and W. S. Noble, “Kernels for gene regulatory regions,” in *Advances in Neural Information Processing Systems*, pp. 1401–1408, 2005.

- [35] D. Lee, R. Karchin, and M. A. Beer, “Discriminative prediction of mammalian enhancers from DNA sequence,” *Genome Research*, vol. 21, pp. 2167–2180, Dec. 2011.
- [36] T. Bailey and C. Elkan, “Fitting a mixture model by expectation maximization to discover motifs in biopolymers.,” in *International Conference on Intelligent Systems for Molecular Biology; ISMB. International Conference on Intelligent Systems for Molecular Biology*, vol. 2, pp. 28–36, 1994.
- [37] J. E. Reid and L. Wernisch, “STEME: efficient EM to find motifs in large data sets,” *Nucleic Acids Research*, vol. 39, pp. e126–e126, Oct. 2011.
- [38] T. L. Bailey, “DREME: motif discovery in transcription factor ChIP-seq data,” *Bioinformatics*, vol. 27, pp. 1653–1659, June 2011.
- [39] A. P. Dempster, N. M. Laird, and D. B. Rubin, “Maximum likelihood from incomplete data via the EM algorithm,” *Journal of the Royal Statistical Society. Series B (Methodological)*, pp. 1 — 38, 1977.
- [40] A. Anandkumar, D. Hsu, F. Huang, and S. M. Kakade, “Learning high-dimensional mixtures of graphical models,” *arXiv preprint arXiv:1203.0697*, 2012.
- [41] B. Boots, S. M. Siddiqi, and G. J. Gordon, “Closing the learning-planning loop with predictive state representations,” *The International Journal of Robotics Research*, vol. 30, no. 7, pp. 954 — 966, 2011.
- [42] B. Balle, W. Hamilton, and J. Pineau, “Methods of moments for learning stochastic languages: Unified presentation and empirical comparison,” in *Proceedings of the 31st International Conference on Machine Learning (ICML-14)* (T. Jebara and E. P. Xing, eds.), pp. 1386–1394, JMLR Workshop and Conference Proceedings, 2014.
- [43] J. Song and K. C. Chen, “Spectacle: Faster and more accurate chromatin state annotation using spectral learning,” *bioRxiv*, 2014.
- [44] S. Arora, R. Ge, and A. Moitra, “Learning topic models-going beyond svd,” in *Foundations of Computer Science (FOCS), 2012 IEEE 53rd Annual Symposium on*, pp. 1—10, IEEE, 2012.
- [45] D. Hsu and S. M. Kakade, “Learning gaussian mixture models: Moment methods and spectral decompositions,” *CoRR*, vol. abs/1206.5766, 2012.
- [46] B. Xie, B. R. Jankovic, V. B. Bajic, L. Song, and X. Gao, “Poly (a) motif prediction using spectral latent features from human DNA sequences,” *Bioinformatics*, vol. 29, no. 13, pp. i316–i325, 2013.

- [47] A. Quattoni, U. EDU, B. Balle, M. CA, X. Carreras, and A. Globerson, “Spectral regularization for max-margin sequence tagging,” 2014.
- [48] J. Y. Zou, D. Hsu, D. C. Parkes, and R. P. Adams, “Contrastive learning using spectral methods,” in *Advances in Neural Information Processing Systems*, pp. 2238–2246, 2013.
- [49] H. Touzet and J.-S. Varre, “Efficient and accurate p-value computation for position weight matrices,” *Algorithms for Molecular Biology*, vol. 2, no. 1, p. 15, 2007.
- [50] T. D. Schneider and R. M. Stephens, “Sequence logos: a new way to display consensus sequences,” *Nucleic Acids Res.*, vol. 18, pp. 6097–6100, Oct. 1990.
- [51] F. Bauer and C. Fike, “Norms and exclusion theorems.,” *Numerische Mathematik*, vol. 2, pp. 137–141, 1960.
- [52] B. W. Bader, T. G. Kolda, and others, *MATLAB Tensor Toolbox Version 2.5*. Jan. 2012. Published: Available online.

A Technical Details

Number of Mixture Components and Grouped Variables When Transcription Factor binding affinities are approximated by product distributions, motif PWM can be identified with the conditional probabilities of a mixture of product distributions and learned using spectral techniques. We associate the primary motifs in the dataset with the mixture components of the smallest relative entropy, where the relative entropy is computed with respect to a background distribution estimated from a control sample. In the case of noisy data, besides such primary motifs a number of non-specific binding sub-sequences as regions containing repeated letters or low-complexity patterns, can also be over-represented in the dataset. Moreover, if the size of the sliding window used to compute the empirical distributions does not match exactly the size of the target motif, strong signals for many shifted versions of the same sub-sequence should be expected. We take these effects into account by defining a preliminary model that includes a number of extra components, to be associated with all secondary motifs in the dataset and shifted replicates in the sliding window records. In other words, we learn a mixture with a high and arbitrary number of components, say $p > 15$, and select the non-trivial models at the end according to their relative entropy computed respect to the background distribution.

A limitation of spectral methods is the fact that, by construction, the size of the sequence alphabet $d = |\mathcal{A}|$ bounds from above the number of components in the mixture, being d the maximum number of

distinct eigenvalues that can be obtained from the spectral decomposition of a $d \times d$ matrix. To overcome this limitation we increase the dimensionality of the alphabet by grouping variables. We can then perform the spectral decomposition in a higher dimensional space. More explicitly, grouped variables of dimension d^n are obtained by reading n contiguous letters as a single character, belonging to the bigger alphabet $\mathcal{A}^{\otimes n}$. Given the length of the sliding window $\ell = 3n$, we define grouped variables of dimension d^n as follows

$$\underbrace{x_1 \cdots x_n}_x \quad \underbrace{x_{n+1} \cdots x_{2n}}_y \quad \underbrace{x_{2n+1} \cdots x_\ell}_z \quad (6)$$

where $x_i \in \mathcal{A}$ and $x, y, z \in \mathcal{A}^{\otimes n}$.

Sliding Window and Joint Empirical Probabilities In the space of grouped variables, given a dataset of sequences \mathcal{S} , the empirical joint distributions are defined by

$$[\hat{P}(x, y, z)]_{i,j,k} = \frac{1}{\mathcal{N}} \sum_{s \in \mathcal{S}} \sum_{i=1}^{|s|-\ell} \delta_{s(i:i+n-1),i} \delta_{s(i+n:i+2n-1),j} \delta_{s(i+2n:i+\ell-1),k} \quad i, j, k = 1, \dots, d^n \quad (7)$$

where $[P(x)]_i$ is the probability of observing $x = i$, \mathcal{N} is a normalization factor, ℓ is the length of the sliding window, δ_{ij} is the Kronecker delta function, and $s(a : b)$, with $1 \leq a \leq b \leq |s|$, denotes a sub-sequence of $s \in \mathcal{S}$ starting at position a and ending at position b inclusive.

We marginalise (7) to obtain the pairwise probability matrices

$$[\hat{P}(x, y)]_{ij} = \sum_{a=1}^{d^n} [\hat{P}(x, y, z)]_{ija} \mathbf{1}_a, \quad [\hat{P}(x, z)]_{ij} = \sum_{a=1}^{d^n} [\hat{P}(x, y, z)]_{iaj} \mathbf{1}_a, \quad i, j = 1, \dots, d^n \quad (8)$$

where $\mathbf{1} = [1, \dots, 1]$ and reduce the triple probability tensor to a matrix via the further contraction

$$[\hat{P}_\theta(x, y, z)]_{ij} = \sum_a [\hat{P}(x, y, z)]_{iaj} \theta_a \quad (9)$$

where θ is an arbitrary vector of dimension d^n .

Tensor Spectral Decomposition Assuming a mixture of product distributions with p mixture components over a space of dimension d^n , pairwise probability matrices and triple probability tensors read

$$P(x, y) = X \text{diag}(h) Y^T \quad P(x, z) = X \text{diag}(h) Z^T \quad [P(x, y, z)]_{ijk} = \sum_{r=1}^p h_r [X]_{ir} [Y]_{jr} [Z]_{kr} \quad (10)$$

where $h = [h_1, \dots, h_p]$ is a vector of mixing weights such that $w \cdot \mathbf{1} = 1$ and $h_r > 0$, for all $r = 1, \dots, p$, and X, Y, Z are $d^n \times p$ matrices whose columns sum to one. As in (9), we reduce the tensor $P(x, y, z)$ to a matrix by contracting its second index to an arbitrary d -dimensional vector θ and obtain

$$P_\theta(x, y, z) = X \text{diag}(h) \text{diag}(\theta^T Y) Z^T \quad (11)$$

where $\text{diag}(h)$ and $\text{diag}(\theta^T Y)$ are diagonal matrices whose p entries are the components of the vectors h and $\theta^T Y$ respectively. When $d^n > p$ it is convenient to reduce the size of the joint probability matrices by means of a low-rank approximation as follows. One assumes the matrices X, Y to have rank p and $h_r > 0$ for all $r = 1, \dots, p$ and defines

$$S_y(\zeta) = V_x^T P_\zeta(x, y, z) V_z (V_x^T P(x, z) V_z)^{-1} = V_x^T X \text{diag}(\zeta^T U_y^T Y) (V_x^T X)^{-1} \quad (12)$$

where

$$[P_\zeta(x, y, z)]_{ij} = \sum_a [P(x, y, z)]_{iaj} [\zeta^T U_y^T]_a \quad (13)$$

ζ is any p -dimensional vector and U_x, U_y, V_x, V_z are the $d^n \times p$ orthogonal matrices defined by

$$\hat{P}(x, y)|_{\text{rank}=p} = U_x \Sigma_{xy} U_y^T, \quad \hat{P}(x, z)|_{\text{rank}=p} = V_x \Sigma_{xz} V_z^T \quad (14)$$

with Σ_{xy}, Σ_{xz} being the diagonal matrices containing the p singular values of $\hat{P}(x, y), \hat{P}(x, z)$. The matrix $S_y(\zeta)$ is called "observable" because it can be estimated directly from the sample using the empirical matrices $\hat{P}(x, y, z)$ and $\hat{P}(x, z)$. Focusing on the eigenvalues of $S_y(\theta)$, relation (12) implies that it is possible, under the model assumption $\text{rank}(X) = p = \text{rank}(Y)$ and $h_r > 0$ for all $r = 1, \dots, p$, to recover the conditional probabilities Y of a mixture of p hidden components over a space of dimension d^n , via the SVD decomposition of two $d^n \times d^n$ matrices and the spectral decomposition of few $p \times p$ matrices (actually one needs exactly p matrices to obtain Y , see below).

Approximate Eigenvalues The empirical estimation of (3) for a given p -dimensional vector ζ is defined as

$$\hat{S}_y(\zeta_i) = V_x^T \hat{P}_\zeta(x, y, z) V_z (V_x^T \hat{P}(x, z) V_z)^{-1}, \quad [\hat{P}_\zeta(x, y, z)]_{ij} = \sum_a [\hat{P}(x, y, z)]_{iaj} [\zeta^T U_y^T]_a \quad (15)$$

When the empirical distributions are not drawn exactly from a mixture of product distributions or the sample size is finite, the eigenvalues and eigenvectors of (15) can contain negative or imaginary parts. A theorem, *Lemma 4 (Eigenvalue Separation)* in [24], states that, for any $0 < \alpha < 1$, an eigenvalues separation of size $\sim \alpha$ is guaranteed with probability at least $1 - \alpha$ if the vector ζ is chosen to be a Gaussian random vector with zero mean and variance one. However, from a more practical point of view, the fact that the eigenvalues spacing and the failure probability are roughly of the same order is often source of instabilities [26].

To increase the stability of our algorithm we choose a set of distinct random vectors ζ_1, \dots, ζ_p and perform an approximate joint diagonalisation of the corresponding nearly-commuting matrices $\hat{S}_y(\zeta_i)$ [27, 25].. Following [28], we compute the Schur decomposition of a linear combination of the nearly commuting

matrices $\hat{S}_y(\zeta_i)$, *i.e.*

$$\hat{S}_y = \frac{1}{p} \sum_i^p \hat{S}_y(\zeta_i) = Q^T \sigma Q, \quad (16)$$

where Q is an orthogonal matrix and σ is upper triangular. The orthogonal matrix Q is then used to compute the conditional probabilities matrix Y by choosing $\zeta_i = \mathbf{e}_i$ for all $i = 1, \dots, p$, where \mathbf{e}_i is a vector with a one in the i th coordinate and zero otherwise. For each $i, j = 1, \dots, p$ we compute

$$\Lambda_{ij}^y = [Q^T \hat{S}_y(\mathbf{e}_i) Q]_{jj} \quad (17)$$

where $\hat{S}(\mathbf{e}_i)$ is defined in (15) (with $\zeta_i = \mathbf{e}_i$), and then obtain $Y = U_y \Lambda^y$. Analogously, we recover X, Z from $X = U_x \Lambda^x$ and $Z = U_z \Lambda^z$ where, for each $i, j = 1, \dots, p$ we calculate

$$\Lambda_{ij}^x = [E_x \hat{S}_x(\mathbf{e}_i) E_x]_{jj}, \quad \Lambda_{ij}^z = [E_z \hat{S}_z(\mathbf{e}_i) E_z]_{jj} \quad (18)$$

with

$$E_x = W_y^T Y, \quad \hat{S}_x(\zeta_i) = W_y^T \hat{P}_{x\zeta}(x, y, z) W_z (W_y^T \hat{P}(y, z) W_z)^{-1}, \quad [\hat{P}_{x\zeta}(x, y, z)]_{ij} = \sum_a [\hat{P}(x, y, z)]_{aij} [\zeta^T U_x^T]_a \quad (19)$$

$$E_z = V_x^T X, \quad \hat{S}_z(\zeta_i) = U_x^T \hat{P}_{z\zeta}(x, y, z) U_y (U_x^T \hat{P}(x, y) U_y)^{-1}, \quad [\hat{P}_{z\zeta}(x, y, z)]_{ij} = \sum_a [\hat{P}(x, y, z)]_{ija} [\zeta^T V_z^T]_a \quad (20)$$

and W_y, W_z defined by

$$\hat{P}(y, z)|_{rank-p} = W_y \Sigma_{yz} W_z^T \quad (21)$$

where Σ_{yz} is the diagonal matrix of singular values of $\hat{P}(y, z)$.

It is possible to relate the error on the obtained eigenvalues to the non-commutativity of the nearly commuting empirical matrices $\hat{S}_y(\zeta_i)$ as follows. Letting $\varepsilon = \max_{i,j} \|\hat{S}_y(\zeta_i) \hat{S}_y(\zeta_j) - \hat{S}_y(\zeta_j) \hat{S}_y(\zeta_i)\|_F$, where $\|A\|_F = \sqrt{\text{Tr}[A^T A]}$, and $\tilde{T}_i = Q^T \hat{S}_y(\zeta_i) Q$ with Q defined in (16), it easy to show that, for all $i = 1, \dots, p$

$$\sigma \tilde{T}_i - \tilde{T}_i \sigma = Q^T E_i Q, \quad E_i = \frac{1}{p} \sum_{j=1}^p (\hat{S}_y(\zeta_j) \hat{S}_y(\zeta_i) - \hat{S}_y(\zeta_i) \hat{S}_y(\zeta_j)) \quad (22)$$

and $\|Q^T E_i Q\|_F \leq \varepsilon$. This implies that $[\tilde{T}_i]_{j,k} = O(\varepsilon)$ for $j > k$, provided that the separation between the eigenvalues of \hat{S}_y is $O(1)$ (see [28] for more details). The error on the eigenvalues is then estimated via the Bauer-Fike theorem [51], using ε as an upper bound for the norm of the perturbation matrix. More precisely, for all $j = 1, \dots, p$ one can find a k such that

$$|\Lambda_{ij}^y - [\zeta_i^T U_y^T Y]_k| \leq \kappa(U_x^T X) \varepsilon \quad \forall i \quad (23)$$

where $\kappa(V) = \|V\| \|V^{-1}\|$.

Higher Dimensional Models and Components Selection The output of the spectral decomposition consists of three $d^n \times p$ matrices X, Y, Z , that contain the conditional probability distributions over the d^n -dimensional space, respectively for the variables (x, y, z) . For each $r = 1, \dots, p$, the columns of X, Y and Z combine to form the higher dimensional PWM's defined by

$$H_r \in [0, 1]^{d^n \times 3} \quad s.t. \quad \begin{cases} [H_r]_{i1} = X_{ir}, & [H_r]_{i2} = Y_{ir}, & [H_r]_{i3} = Z_{ir} \\ \sum_i [H_r]_{ik} = 1 & \forall k \end{cases} \quad (24)$$

For all $r = 1, \dots, p$ we compute the relative entropy of H_r and choose the models corresponding to the p_{top} smallest values. The relative entropy is given by

$$I(r) = \sum_{i=1}^{d^n} \sum_{k=1}^3 [H_r]_{ik} \log \left(\frac{[H_r]_{ik}}{B_{ik}} \right) \quad (25)$$

for $r = 1, \dots, p$, where B is a background distribution defined by

$$B_{i1} = \sum_{j,k=1}^{d^n} [\hat{P}_b(x, y, z)]_{ijk} \mathbf{1}_j \mathbf{1}_k, \quad B_{i2} = \sum_{j,k=1}^{d^n} [\hat{P}_b(x, y, z)]_{jik} \mathbf{1}_j \mathbf{1}_k, \quad B_{i3} = \sum_{j,k=1}^{d^n} [\hat{P}_b(x, y, z)]_{jki} \mathbf{1}_j \mathbf{1}_k \quad (26)$$

with $\mathbf{1}$ being a d^n -dimensional vectors of ones and $\hat{P}_b(x, y, z)$ the empirical triple probability tensor computed using (7) for the control dataset. In particular, we define the control sample C to be a random selection of DNA fragments bounded by a different transcription factor. This is a good background choice because allows one to exclude a number of non-specific bounding motifs, expected to be similar in all experiments.

Low Dimensional PWM's and Threshold Selection According to their relative entropies, p_{top} higher-dimensional models H_r^{top} are selected and used to obtain the corresponding low-dimensional frequency matrices h_r^{top} , that contain the binding probability over the original alphabet \mathcal{A} . Instead of marginalizing the grouped conditional probabilities in each H_r^{top} , we use the high-dimensional models to obtain various sub-sequences alignments from the sample \mathcal{S} and then compute the corresponding h_r^{top} by counting the occurrences of the d -dimensional characters at every position x_1, \dots, x_ℓ .

More precisely, for each model $r = 1, \dots, p_{\text{top}}$, we assign a score to all length- ℓ sub-sequences in the dataset \mathcal{S} using the scoring function

$$f_{\text{alignment}}(s_\ell, r) = \log([H_r^{\text{top}}]_{s_\ell(1:n-1)1}) + \log([H_r^{\text{top}}]_{s_\ell(n:2n-1)2}) + \log([H_r^{\text{top}}]_{s_\ell(2n:\ell)3}) \quad (27)$$

where s_ℓ is a sub-sequence of length ℓ in \mathcal{S} and $s_\ell(a:b)$ for $1 \leq a \leq b \leq \ell$ is the string $[s_\ell(a), s_\ell(a+1), \dots, s_\ell(b-1), s_\ell(b)]$, with $s(i)$ denoting the i th element of s_ℓ . For $r = 1, \dots, p_{\text{top}}$, we include in the r th alignment the sub-sequences that satisfy $f_{\text{alignment}}(s_\ell, r) > \xi$, where ξ is a threshold chosen out of a finite set $\{\xi_1, \dots, \xi_N\}$

in order to maximise the information content of the model. More explicitly, for every threshold value ξ in a finite set $\{\xi_1, \xi_2, \dots, \xi_N\}$, where N is an input parameter, we compute a d -dimensional frequency matrices defined by

$$[h_r^{\text{top}}(\xi)]_{i,j} = \sum_{s_\ell \in S(\xi)} \delta_{i,s(i+j-1)}, \quad S(\xi) = \{s_\ell \in \mathcal{S} \mid f_{\text{alignment}}(s_\ell, r) > \xi\} \quad (28)$$

and evaluate the information content of the model using

$$R_r(\xi) = \sum_{k=1}^{\ell} [2 - (E_r(\xi, k) + \varepsilon_r(\xi, k))] \quad (29)$$

where the entropy $E_r(\xi, k)$ and the small sample correction $\varepsilon_r(\xi, k)$ are

$$E_r(\xi, k) = - \sum_{i=1}^d \frac{[h_r^{\text{top}}(\xi)]_{i,k}}{\sum_i [h_r^{\text{top}}(\xi)]_{i,k}} \log \left(\frac{[h_r^{\text{top}}(\xi)]_{i,k}}{\sum_i [h_r^{\text{top}}(\xi)]_{i,k}} \right), \quad \varepsilon_r(\xi, k) = \frac{d-1}{2 \log(2)} \frac{1}{\sum_i [h_r^{\text{top}}(\xi)]_{i,k}} \quad (30)$$

Finally, we define the most informative model to be $h_{r^*}^{\text{top}}(\xi^*)$, with

$$(r^*, \xi^*) = \arg \max_{r, \xi} R_r(\xi), \quad r = 1, \dots, p_{\text{top}}, \quad \xi \in \{\xi_1, \xi_2, \dots, \xi_N\} \quad (31)$$

and compute its logo using the application `weblogo` available at <http://weblogo.berkeley.edu/> [50].

Note that in the case of stochastic models, the problem of defining an optimal matching threshold given a desired minimal statistical significance of the selected instances (usually in terms of P-value) is an NP-hard problem (see for example [49]). We herein propose a heuristic solution to this problem. Improvements to this heuristic go beyond the scope of the current work and will be subject of future studies.

B Algorithms

Main algorithm

Input: dataset \mathcal{S} of sequences over alphabet \mathcal{A} , number of mixture components p , group size n , control dataset C , threshold values $\xi = \xi_1, \dots, \xi_N$,

- use a sliding window of length $\ell = 3n$ to compute $3n$ -mers occurrences from \mathcal{S}
- convert grouped characters to index and form the sparse tensor $\hat{P}(x, y, z)$ from a coordinates matrix with rows

$$\text{index}_x \quad \text{index}_y \quad \text{index}_z \quad \text{value}$$

where $1 \leq \text{index}_a \leq |\mathcal{A}|^n$ for $a = x, y, z$

- repeat the previous steps using C instead of \mathcal{S} to obtain $\hat{P}_b(x, y, z)$ and compute the background conditional distributions B using (26)
 - decompose $\hat{P}(x, y, z)$ using *Spectral Algorithm* to obtain H_r , for $r = 1, \dots, p$
 - for $r = 1, \dots, p$ compute the relative entropy of H_r using (25)
 - select the p_{top} components H_r^{top} with smallest relative entropy
 - **for** $r = 1, \dots, p_{\text{top}}$
 - **for** $\xi = \xi_1, \dots, \xi_N$
 - * compute frequency matrix $h_r^{\text{top}}(\xi)$ using (28)
 - * compute the associated information content $R(r, \xi)$ using (29)
 - **end for**
 - **end for**
 - let $(r^*, \xi^*) = \arg \max_{r, \xi} R(r, \xi)$
 - compute the logo of $h_{r^*}^{\text{top}}(\xi^*)$ using `weblogo`
- Output:** Position Weight Matrix of the Transcription Factor binding site and corresponding logo

Spectral Algorithm

Input: coordinates matrix for the $d^n \times d^n \times d^n$ joint probability tensor $\hat{P}(x, y, z)$, number of mixture components p

- compute the sparse tensor $\hat{P}(x, y, z)$ from the coordinates matrix and the pairwise probability matrices $\hat{P}(x, y), \hat{P}(x, z), \hat{P}(y, z)$ by contracting to $\mathbf{1}$ on the third, second and first index respectively²
- compute the rank- p approximation

$$\hat{P}(x, y)|_{\text{rank-}p} = U_{xy} \Sigma_{xy} V_{xy}^T, \quad \hat{P}(x, z)|_{\text{rank-}p} = U_{xz} \Sigma_{xz} V_{xz}^T, \quad \hat{P}(y, z)|_{\text{rank-}p} = U_{yz} \Sigma_{yz} V_{yz}^T \quad (32)$$

- **for** $i = 1, \dots, p$
 - draw a random p -dimensional vector θ and define $v = V_{xy} \theta$

²We have used the online available package MATLAB Tensor Toolbox [52] for all tensors manipulation.

- define $[\hat{P}_v(x, y, z)]_{ik} = \sum_j [\hat{P}(x, y, z)]_{ijk} v_j$
- form $M_v = U_{xz}^T \hat{P}_v(x, y, z) V_{xz} (U_{xz}^T \hat{P}(x, z) V_{xz})^{-1}$
- let $M = M + M_v$

end for

- compute the Schur decomposition $M = QSQ^T$
- **for** $r = 1, \dots, p$
 - let $v = V_{xy}(:, r)$
 - define $[\hat{P}_v(x, y, z)]_{ik} = \sum_j [\hat{P}(x, y, z)]_{ijk} v_j$
 - form $M_v = U_{xz}^T \hat{P}_v(x, y, z) V_{xz} (U_{xz}^T \hat{P}(x, z) V_{xz})^{-1}$ and compute $S_v = Q^T M_v Q$
 - let $L(r, i) = S_v(i, i)$

end for

- let $Y = (V_{xy}L)^+$ and normalize the columns of Y to 1
- let $E = U_{yz}^T Y$
- **for** $r = 1, \dots, p$
 - let $v = U_{xy}(:, r)$
 - define $[\hat{P}_v(x, y, z)]_{jk} = \sum_i [\hat{P}(x, y, z)]_{ijk} v_i$
 - form $M_v = U_{yz}^T \hat{P}_v(x, y, z) V_{yz} (U_{yz}^T \hat{P}(y, z) V_{yz})^{-1}$ and compute $D_v = (E)^{-1} M_v E$
 - let $L(r, i) = D_v(i, i)$

end for

- let $X = (U_{xy}L)^+$ and normalize the columns of X to 1
- let $E = U_{xy}^T X$
- **for** $r = 1, \dots, p$
 - let $v = V_{xz}(:, r)$
 - define $[\hat{P}_v(x, y, z)]_{ij} = \sum_k [\hat{P}(x, y, z)]_{ijk} v_k$

- form $M_v = U_{xy}^T \hat{P}_v(x, y, z) V_{xy} (U_{xy}^T \hat{P}(x, y) V_{xy})^{-1}$ and compute $D_v = (E)^{-1} M_v E X$
- let $L(r, i) = D_v(i, i)$

end for

- let $Z = (V_{xz} L)^+$ and normalize the columns of Z to 1

Output: Position Weight Matrix $H_r \in [0, 1]^{d^n \otimes 3}$, for $r = 1, \dots, p$